Proceedings of the
International Conference on Mechanical Engineering and Renewable Energy 2019
(ICMERE2019) 11 – 13 December, 2019, Chittagong, Bangladesh

ICMERE2019-PI-153

EFFECT OF DENSITY, DYNAMIC VISCOSITY, VELOCITY, AND DIAMETER ON WALL SHEAR STRESS FOR TURBULENT PIPE FLOW

Abu Raihan Ibna Ali[1*], Bodius Salam[2], Moham Ed Abdur Razzaq[3], Jamal Uddin Ahamed[4], Tafsirul Hassan[5], and Md. Fahim Bin Karim[6]

[1] Department of Mechanical Engineering, Chittagong University of Engineering & Technology, Chittagong-4349, Bangladesh
abu.raihan.pilu@gmail.com*, bsalam@cuet.ac.bd , a.razzaq@cuet.ac.bd , jamal@cuet.ac.bd , tafsir2086@gmail.com , fahim0797@gmail.com

Abstract- *In growing engineering disciplines and arterial fluid mechanics, Wall Shear Stress (WSS) plays an important role in fluid flow. This tangential force exerted on the boundary wall is also important in skin drag reduction. The objective of the present study is to explore the relation of wall shear stress among the diameter of the pipe, velocity, density and dynamic viscosity of the fluid. Investigation was carried out for water flow through the pipes using ANSYS FLUENT (Academic Version). Wall Shear Stress was observed both for full length of the tube and fully developed flow condition. It is concluded that wall shear stress in pipe flow is proportional to velocity, density and dynamic viscosity of fluid but inversely proportional to the diameter of the pipe.*

Keywords: Wall Shear Stress, WSS, Turbulent Flow, Skin Friction

1. INTRODUCTION

In fluid flow over a solid boundary, shear stress varies from wall to centerline which is maximum at wall and zero at the centerline. The maximum stress at the wall is known as wall shear stress. The tangential force exerted by the flowing fluid (real fluid, μ>0) along the solid boundary in the opposite direction of flow incur a shear stress on that boundary which is known as wall shear stress (WSS). It can be used to characterize the strength of flow. Wall shear stress for turbulent flow is defined by,

$$\tau_w = \left(\mu\frac{\partial u}{\partial y} + \eta\frac{\partial u}{\partial y}\right)_{y=0} \quad (1)$$

Where, μ= dynamic viscosity
u = velocity of the fluid along the boundary
η= eddy viscosity

Here, $\mu\frac{\partial u}{\partial y}$ is shear stress due to viscosity and $\eta\frac{\partial u}{\partial y}$ is shear stress due to turbulence. η can be written as ρε, where ε is called eddy diffusion coefficient. In turbulent flow, eddy viscosity is much larger than molecular viscosity except near the solid boundary. Turbulent momentum transport is dominant over molecular momentum transport everywhere except at solid boundary. From Eq. (1), WSS can be expressed as the function of fluid velocity, the diameter of the pipe, the density of fluid and viscosity of the fluid.

WSS can also be calculated from the friction factor as,

$$\tau_w = \frac{\rho C_f V^2}{2} \quad (2)$$

The skin friction coefficient can be estimated from Patel's correlation [1] for pipe flow as,

$$f = 0.316Re^{-\frac{1}{4}} \quad (3)$$

Another correlation widely used for smooth pipe flow is Petukhov [2] correlation as,

$$f = (1.82\log Re - 1.64)^{-2} \quad for\ 3000 < Re < 5\times 10^6 \quad (4)$$

Alternatively, for fully developed turbulent pipe flow, friction factor can be calculated iteratively from the Colebrook equation [3]. Colebrook equation shows that the friction factor depends on the Reynolds number and the relative roughness ε /D.

$$\frac{1}{\sqrt{f}} = -2.0\log\left(\frac{\frac{\varepsilon}{D}}{3.7} + \frac{2.51}{Re\sqrt{f}}\right) \quad (5)$$

The friction factor is four times of skin friction coefficient, $f = 4C_f$. (6)

Wall shear stress (WSS) has great importance in the field of aerodynamics and fluid mechanics from the fact that the integrated value of WSS is the viscous component of total drag. Drag or skin friction can be optimized by determination of the wall shear stress in aerodynamics. In the case of underwater vehicles like a submarine, WSS contributes to increasing frictional drag up to 90% of total drag. Park et al [4] investigated to control WSS by the method of wall blowing and suction. It is also an important determinant to characterize flow conditions. Because of high WSS produced by multiphase flow, protective corrosion layer may damage and leads to corrosion. [5]

It also plays a significant role in arterial fluid mechanics. Medical science has found a direct relationship of WSS that act on the artery wall to the development of cardiovascular disease atherosclerosis which is a complex disease that causes a progressive occlusion of the arteries. [6]

WSS is difficult to measure directly as measuring the shear stress and velocity gradient on the boundary layer is not easy. In the arterial system, WSS is determined from ultrasound velocity measurements which are extrapolated to the wall and then WSS is measured from wall shear rate. In aerodynamics, WSS is often measured using compact strain gauges. Gijsen et al [7] determined WSS from the deformation of an elastic gel layer inside the flow model. Floating element sensor method was successfully used to measure WSS by Li et al. [8]

WSS is found in the viscous sublayer portion. The viscous sublayer is a thin layer (a fraction of a millimeter to many millimeters) of the boundary layer. In viscous sublayer, viscous shear stress predominates over turbulent shear stress. Generally, the thickness of this layer depends on the characteristics of the fluid and its flow. Viscous sublayer often checked from a dimensionless number measured of distance from the boundary by $\frac{\rho^{\frac{1}{2}}\tau_0^{\frac{1}{2}}y}{\mu}$ denoted by y+. In order to measure WSS, it important to check y+ value in simulation. y+ value for the transition from the viscous sublayer to the buffer layer is about 5, and the transition from the buffer layer to the turbulent layer is about 30. Hence, it is important to cluster mesh near the boundary.

2. MATERIALS AND METHODS

2.1 Physical model

2D axisymmetric pipes having a length of 2m and diameter of 0.01m, 0.02m, 0.03m, 0.04m, 0.05m, and 0.06m were modeled and simulated in ANSYS for different density and dynamic viscosity. Boundary conditions were applied and solved numerically. The fluid flowing in the pipe is water which has properties described in Table 1.

2.2 Mathematical modeling and data reduction

2.2.2 Governing Equation

Conservation of Mass:

continuity equation in differential form is

$$\frac{\partial \rho}{\partial t} + \vec{\nabla}.\left(\rho\vec{\mathrm{V}}\right) = S_m \quad (7)$$

For 2D axisymmetric geometries,

$$\frac{\partial \rho}{\partial t} + \frac{\partial}{\partial x}(\rho v_x) + \frac{\partial}{\partial r}(\rho v_r) + \frac{\rho v_r}{r} = S_m \quad (8)$$

Conservation of mass equation is also known as continuity equation.

Conservation of Momentum:

Conservation of momentum in an inertial (non-accelerating) reference frame is described by,

$$\frac{\partial}{\partial t}\left(\rho\vec{\mathrm{V}}\right) + \nabla.(\rho\vec{\mathrm{v}}\vec{\mathrm{v}}) = -\nabla \mathrm{p} + \nabla.(\bar{\bar{\tau}}) + \rho\vec{\mathrm{g}} + \vec{\mathrm{F}} \quad (9)$$

Stress tensor is given by

$$\bar{\bar{\tau}} = \mu\left[(\nabla\vec{\mathrm{v}} + \nabla\vec{\mathrm{v}}^T) - \frac{2}{3}\nabla.\vec{\mathrm{v}}I\right] \quad (10)$$

For 2D axisymmetric geometry conservation of momentum equation is as,

Axial and radial momentum conservation equations are given by,

$$\frac{\partial}{\partial t}(\rho v_x) + \frac{1}{\mathrm{r}}\frac{\partial}{\partial x}(r\rho v_x v_x) + \frac{1}{\mathrm{r}}\frac{\partial}{\partial r}(r\rho v_r v_x) = -\frac{\partial p}{\partial x} + \frac{1}{r}\frac{\partial}{\partial x}\left[r\mu\left(2\frac{\partial v_x}{\partial x} - \frac{2}{3}(\nabla.\vec{\mathrm{v}})\right)\right] + \frac{1}{r}\frac{\partial}{\partial r}\left[r\mu\left(\frac{\partial v_x}{\partial r} + \frac{\partial v_r}{\partial x}\right)\right] + F_x \quad (11)$$

And

$$\frac{\partial}{\partial t}(\rho v_r) + \frac{1}{\mathrm{r}}\frac{\partial}{\partial x}(r\rho v_x v_r) + \frac{1}{\mathrm{r}}\frac{\partial}{\partial r}(r\rho v_r v_r) = -\frac{\partial p}{\partial r} + \frac{1}{r}\frac{\partial}{\partial x}\left[r\mu\left(\frac{\partial v_r}{\partial x} + \frac{\partial v_x}{\partial r}\right)\right] + \frac{1}{r}\frac{\partial}{\partial r}\left[r\mu\left(2\frac{\partial v_r}{\partial r} - \frac{2}{3}(\nabla.\vec{\mathrm{v}})\right)\right] - 2\mu\frac{v_r}{r^2} + \frac{2}{3}\frac{\mu}{r}(\nabla.\vec{\mathrm{v}}) + \rho\frac{v_z^2}{r} + F_r \quad (12)$$

Where,

$$\nabla.\vec{\mathrm{v}} = \frac{\partial v_x}{\partial r} + \frac{\partial v_r}{\partial r} + \frac{v_r}{r} \quad (13)$$

And v_z is the swirl velocity

p = static pressure

$\bar{\bar{\tau}}$ Stress tensor

$\rho\vec{\mathrm{g}}$ = gravitational force

$\vec{\mathrm{F}}$ = external body force

μ= molecular viscosity

I = unit tensor

2.2.2 Turbulence Model

Standard k-ε model is the most widely-used engineering turbulence model which is robust and reasonably accurate. It is a semi-empirical model based on transport equations for turbulence kinetic energy and turbulent dissipation rate. Transport equation of k is derived from the exact equation, while the transport equation for ε is derived using physical reasoning. Standard k-ε model is valid only for fully developed turbulent flows. Enhanced wall function was used as ε equation contains a term which cannot be calculated without wall function.

Transport equation for turbulent kinetic energy (k) is as,

$$\frac{\partial(\rho k)}{\partial t} + \frac{\partial(\rho k u_i)}{\partial x_i} = \frac{\partial}{\partial x_j}\left[\left(\mu + \frac{\mu_t}{\sigma_k}\right)\frac{\partial k}{\partial x_j}\right] + G_k + G_b - \rho\varepsilon - Y_M + S_k \quad (14)$$

And transport equation for turbulent dissipation rate (ε) is as,

$$\frac{\partial(\rho\varepsilon)}{\partial t} + \frac{\partial(\rho\varepsilon u_i)}{\partial x_i} = \frac{\partial}{\partial x_j}\left[\left(\mu + \frac{\mu_t}{\sigma_\varepsilon}\right)\frac{\partial \varepsilon}{\partial x_j}\right] + C_{1\varepsilon}\frac{\varepsilon}{k}(G_k + C_{3\varepsilon}G_b) - C_{2\varepsilon}\rho\frac{\varepsilon^2}{k} + S_\varepsilon \quad (15)$$

Where, $\mu_t = \text{Turbulent viscosity} = \rho C_\mu \frac{k^2}{\varepsilon}$ (16)

G_k = Generation of the turbulent kinetic energy due to the mean velocity gradient

σ_k = Effective Prandtl number for turbulent kinetic energy

σ_ε = Effective Prandtl number for rate of dissipation

$C_{1\varepsilon}, C_{2\varepsilon}$ are constants

Model Constants:
The default values of model constants $C_{1\varepsilon}, C_{2\varepsilon}, C_\mu, \sigma_k, and\ \sigma_\varepsilon$ determined from experiments for fundamental turbulent flows and have the following values
$C_{1\varepsilon} = 1.44, C_{2\varepsilon} = 1.92, C_\mu = 0.09, \sigma_k = 1.0, \sigma_\varepsilon = 1.3$

2.3 Boundary conditions

To study the effect of velocity on WSS, inlet velocity of water was selected as 0.6 m/s, 0.5 m/s, 0.4 m/s, 0.3 m/s, 0.2 m/s and 0.1 m/s at temperature of 300K when diameter and length were 0.6m, 2m respectively. Again, velocity was kept 0.6m/s while diameter was changed to 0.6m, 0.5m, 0.4m, 0.3m, 0.2m and 0.1m at a temperature of 300K to study the relationship of WSS and diameter. Finally, simulations were performed for different density and dynamic viscosity of water (specified in table 1) at different temperature for the diameter of 0.6m and length of 2m. Turbulent intensity is calculated from the Eq. (17)

$$I = \frac{u'}{u_{avg}} = 0.16\, Re_{D_H}^{-\frac{1}{8}} \qquad (17)$$

Table 1: Properties of water

Temperature, T [°C]	Density ρ [kg/m^3]	*Dynamic viscosity* μ [kg/m·s]
5	999.9	1.519×10^{-3}
25	997	0.981×10^{-3}
40	992.1	0.653×10^{-3}
50	988.1	0.547×10^{-3}

2.4 Solution method and convergence criteria

The pipe flow was gravity independent as it was horizontal and steady state. The solver was pressure based and enhanced near wall treatment was selected. Simple scheme solution method was chosen. Under spatial discretization, the gradient was Green Gauge Cell-based and second-order upwind was selected for continuity and turbulent kinetic energy. The values of other parameters under relaxation were the default. Simulations were performed till continuity, k and epsilon residue reached $9.2642 \times 10^{-5}, 5.6870 \times 10^{-5}\ and\ 9.2814 \times 10^{-5}$. Computer with 8 GB DDR4 RAM, Intel(R) Core(TM) i5-6200U CPU @ 2.30GHz (4 CPUs) processor and 2 GB NVIDIA GEFORCE graphics card were used.

2.5 Model validation

2.5.1 Grid Sensitivity Check

Simulations were performed for a different number of mesh elements using maximum face size of 0.2mm, 0.3mm and 0.4mm. Mesh were clustered near the pipe wall to detect viscous sublayer. Grid sensitivity was checked by the numerical value of wall shear stress for inlet velocity of 0.6 m/s. Fig.1 illustrates that WSS increases 1.97% and 3.04% for face size of 0.3 mm and 0.4mm compared with 0.2 mm. So, considering computational cost and accuracy, maximum face size of 0.3mm was selected for the simulations

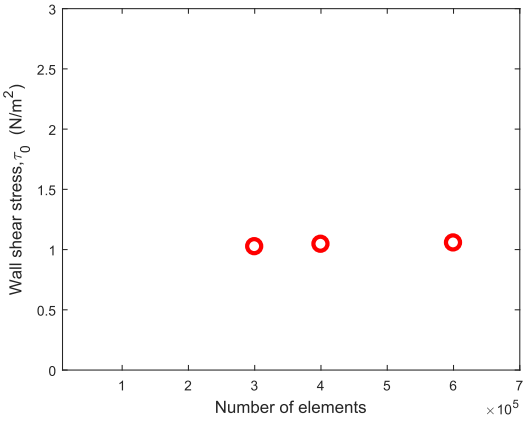

Fig. 1: Wall Shear Stress for a different number of elements

2.5.1 Validation of simulation

The simulation was validated by comparing the friction factor for fully developed pipe (diameter of 0.06m) flow by Petukhov [2] and Patel's [1] correlation. Simulated friction factor showed satisfactory agreement comparing with Petukhov correlation with variation ranging of 0.9% to 7.9%. On the other hand, comparing by Patel's correlation of friction factor showed satisfactory agreement with variation ranging of 2.65% to 6%. Simulation validation is illustrated in fig. 2.

3. EFFECT OF VELOCITY, DIAMETER, AND KINEMATIC VISCOSITY ON WALL SHEAR STRESS

Effect of pipe diameter and fluid velocity are significant on wall shear stress because of affecting the rate of shear in the flow. Effect of fluid density must be considered there must be local fluid acceleration if the flow is turbulent. And another most important fluid property is dynamic viscosity as its role is significant at viscous shear stress at the boundary. So, wall shear stress can be treated as a function of these four variables D, U, ρ, and μ. WSS also depends on axial and transverse tube configuration and on the types of flow.

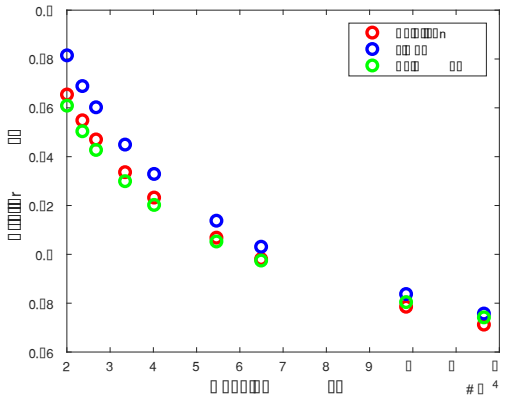

Fig. 2: Relation Between Friction Factor and Reynold number

Fig. 2 illustrates the effect of Reynolds number on the friction factor. Simulated data have been compared with Patel correlation and Petukhov (1970) correlation. Simulated data satisfy both correlations. From Fig. 2, it is observed that the friction factor is inversely proportional to Reynolds number. Consequently, the skin friction coefficient decreases as friction factor is four times of skin friction coefficient. Skin friction coefficient is a dimensionless boundary shear stress which is one kind of flow resistance coefficient.

3.1 Velocity Effect on Wall Shear Stress

Six pipe models were simulated to observe the relation between velocity and wall shear stress for different velocities with constant length of 2 m, the diameter of 0.06 m, density of 997 kg/m^3 and dynamic viscosity of 0.981 × 10^{-3} kg/m·s. Velocities of fluid were selected as 0.1 m/s, 0.2 m/s, 0.3 m/s, 0.4 m/s, 0.5 m/s and 0.6 m/s.

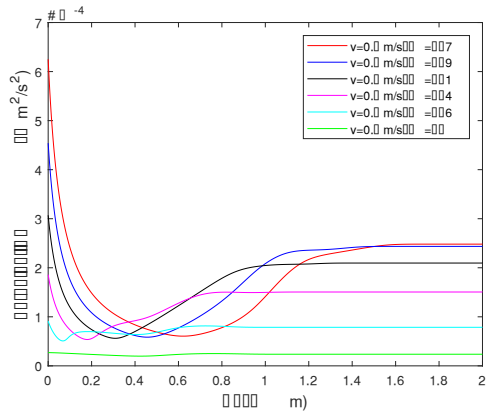

Fig. 3: Turbulent Kinetic Energy for Different Velocity at pipe axis

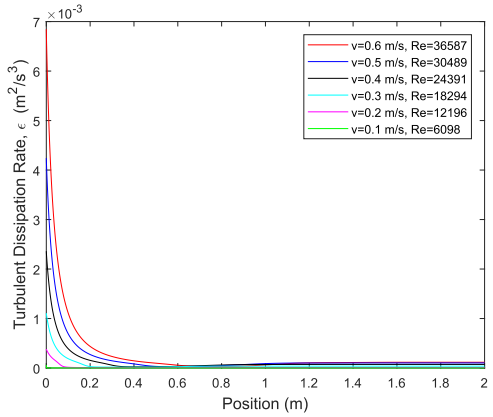

Fig. 4: Turbulent Dissipation Rate for Different Velocity at pipe axis

Turbulent kinetic energy is characterized by the root mean square of velocity fluctuations. And turbulent dissipation is the rate at which turbulence kinetic energy is converted into thermal internal energy. At centerline of fully developed pipe flow, Fig. 3 and Fig. 4 illustrate that turbulent kinetic energy and turbulent dissipation rate increases with the increase in fluid velocity while other parameters are constant.

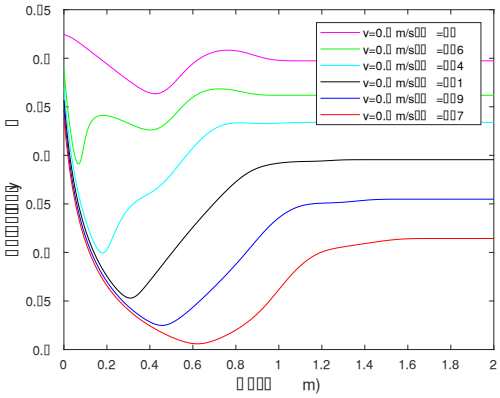

Fig. 5: Turbulent Intensity for Different Velocity at pipe axis

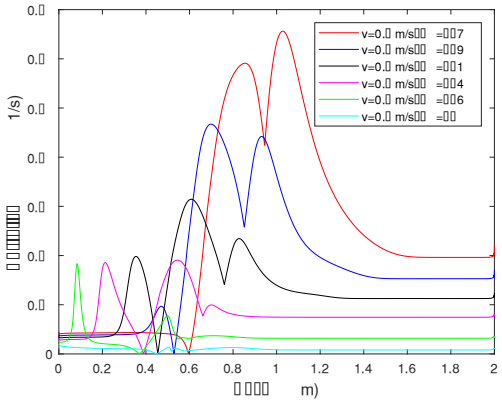

Fig. 6: Vorticity Magnitude for Different Velocity at pipe axis

Turbulent intensity is the ratio of root-mean-square of root mean square of the velocity fluctuations to the mean flow velocity. Fig. 5 illustrates that the percentage of turbulent intensity decreases with the increase in velocity of fluid while Fig. 6 illustrates that vorticity increases

with the increase in fluid velocity. Wall shear stress is associated with the near wall vortices. Hence WSS increases with the increase in vorticity.

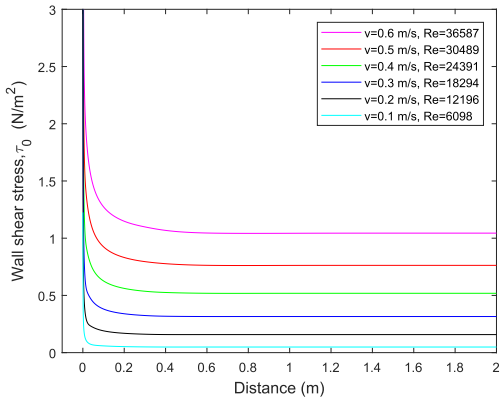

Fig. 6: Local Wall Shear Stress for Different Velocity (full length)

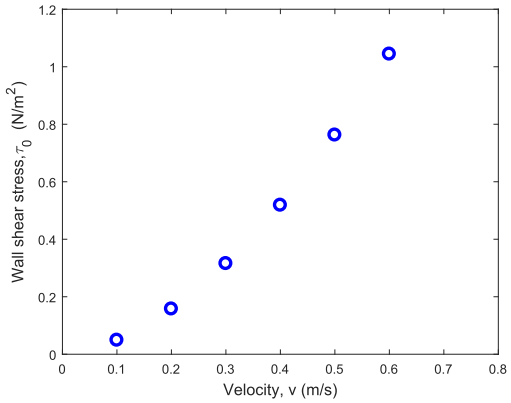

Fig. 7: Wall Shear Stress for Different Velocity Velocity (fully developed flow)

Fig. 6 and Fig. 7 explain the effect of velocity on wall shear stress. From Fig 6 it is observed that wall shear stress is initially very high but after fully developed flow, it becomes constant. Because of low velocity gradient, WSS is initially high. Fig. 7 illustrates that for a fully developed flow, WSS is proportional to the fluid velocity. It increases with the increase in the velocity of the fluid. It is also observed that after certain velocity WSS increases much with the little increase in fluid velocity.

3.2 Diameter Effect on Wall Shear Stress

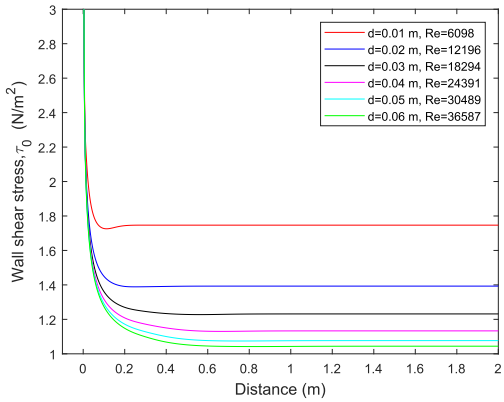

Fig. 8: Local Wall Shear Stress for Different Diameter of Pipe (full length)

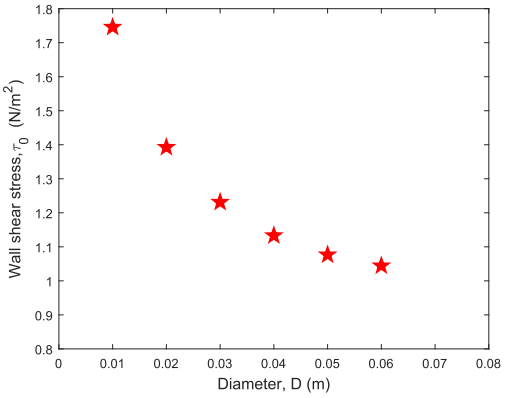

Fig. 9: Wall Shear Stress for Different Diameter of Pipe (fully developed flow)

Another six pipe models were simulated to observe the relation between diameter and wall shear stress for different diameter with a constant velocity of 0.6 m/s, length of 2 m, the density of 997 kg/m^3 and dynamic viscosity of 0.981 × 10^{-3} kg/m·s. Diameter of pipes were selected as 0.01 m, 0.02 m, 0.03m, 0.04m, 0.05m and 0.06m. Fig. 8 and Fig. 9 explain the effect of the increase in diameter on wall shear stress. From Fig 8, it is observed that wall shear stress is initially very high but after fully developed flow, it becomes constant. Because of low velocity gradient, WSS is initially high. Fig. 9 illustrates that for a fully developed flow, WSS is inversely proportional to the diameter of the pipe. It decreases with the increase in the diameter of the pipe.

3.3 Density and Dynamic Viscosity Effect on Wall Shear Stress

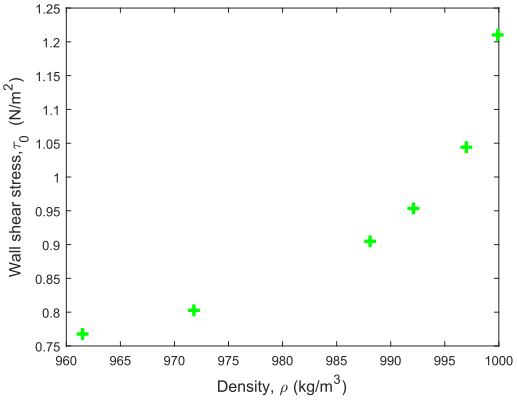

Fig. 10: Wall Shear Stress for Different Fluid Density (fully developed flow)

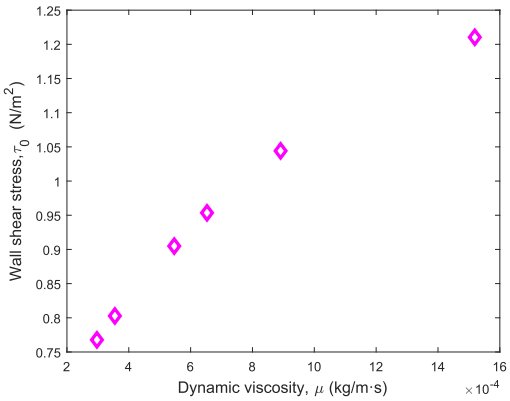

Fig. 11: Wall Shear Stress for Different Dynamic Viscosity (fully developed flow)

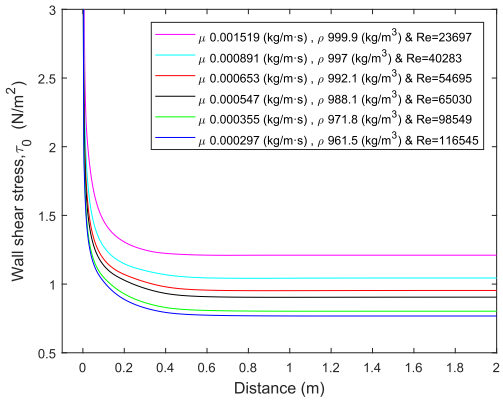

Fig. 12: Local Wall Shear Stress for Different Density and Dynamic Viscosity (fully developed flow)

Six pipe models were simulated to observe the relation between density and dynamic viscosity with wall shear stress for the pipe diameter of 0.06m with a constant velocity of 0.6 m/s, length of 2 m. Density of fluid were selected as 961.5 kg/m^3, 971.8 kg/m^3, 988.1 kg/m^3, 992.1 kg/m^3, 997 kg/m^3 and 999.9 kg/m^3. And dynamic viscosity of fluid was selected as 0.000297 kg/m.s, 0.000355 kg/m.s, 0.000547 kg/m.s, 0.000653 kg/m.s, 0.000891 and 0.001519 kg/m.s. Fig. 10 illustrates the effect of the increase in density on wall shear stress. And Fig 11 illustrates the effect of dynamic viscosity on wall shear stress. From Fig. 12, it is observed that wall shear stress is initially very high but after fully developed flow, it becomes constant. Because of low velocity gradient, WSS is initially high.

5. CONCLUSION

The present work investigated the relationship of wall shear stress (WSS) among fluid velocity, the diameter of the pipe, fluid density and dynamic viscosity. For fully developed pipe flow, the findings of the study are:

- Wall shear stress (WSS) is proportional to the fluid velocity. WSS increases with the increase in fluid velocity when the diameter of the pipe, fluid density, and dynamic viscosity are constant.
- Wall shear stress (WSS) is inverse proportional to the fluid velocity. WSS decreases with the increase in diameter of the pipe when fluid velocity, fluid density, and dynamic viscosity are constant.
- Wall shear stress (WSS) is proportional to the fluid density and dynamic viscosity. WSS increases with the increase in density of fluid when fluid velocity and diameter are constant.

7. REFERENCES

[1] V.C. Patel, "Some Observations on Skin Friction and Velocity Profiles in Fully Developed Pipe and Channel Flows", *J. Fluid Mech.*, vol. 38, no. 1, pp. 181-201, 1969.

[2] B.S. Petukhov, "Heat Transfer and Friction in Turbulent Pipe Flow with Variable Physical Properties", *Advances in heat transfer,* vol. 6, pp. 503–564, 1970.

[3] C. F. Colebrook, "Turbulent Flow in Pipes, with Particular Reference to the Transition between the Smooth and Rough Pipe Laws", *Journal of the Institute of Civil Engineers,* vol. 12, no. 8, pp. 393–422, 1939.

[4] Y. S. Park, S. H. Park, and H. J. Sung, "Measurement of local forcing on a turbulent boundary layer using PIV." *Experiments in Fluids*, Vol. 34, pp. 697-707, 2004.

[5] G. Schmitt and M. Mueller "Critical Wall Shear Stresses in CO2 Corrosion of Carbon Steel." CORROSION 99, NACE International, no. 44, 1999.

[6] K. S. Cunningham and A. I. Gotlieb, "The role of shear stress in the pathogenesis of atherosclerosis." *Laboratory investigation*, Vol. 85, no. 1, pp. 9, 2005.

[7] F. J. H. Gijsen, A. Goijaerts, F. N. Van de Vosse, and J. D. Janssen, "A new method to determine wall shear stress distribution", *Journal of Rheology,* vol. 41, no. 5, pp. 995–1006, 1997.

[8] W. Li, Y. Xiong, B. Brown, K. E. Kee, and S. Nesic, "Measurement of wall shear stress in multiphase flow and its effect on protective FeCO3 corrosion product layer removal", *CORROSION/2015,* 2015.

8. NOMENCLATURE

Symbol	Meaning	Unit
τ_w	Area	(m^2)
u	Velocity of fluid	(m/s)
f	Friction factor	Dimensionless
C_f	Skin friction coefficient	Dimensionless
D	Diameter	m
ε /D	Relative roughness	
Re	Reynolds number	Dimensionless
η	Eddy viscosity	
ρ_{nf}	Density	Kg/m^3
μ	Dynamic viscosity	N.s/m^2